ACS Catalysis

RESEARCH ARTICLE

pubs.acs.org/acscatalysis

Ligand-Induced Drastic Enhancement of Catalytic Activity of Nano-$BiFeO_3$ for Oxidative Degradation of Bisphenol A

Nan Wang,[†] Lihua Zhu,[*,†] Ming Lei,[†] Yuanbin She,[‡] Meijuan Cao,[‡] and Heqing Tang[*,†,$]

[†]College of Chemistry and Chemical Engineering, Huazhong University of Science and Technology, Wuhan 430074, P.R. China

[‡]College of Environmental and Energy Engineering, Beijing University of Technology, Beijing, 100124, P. R. China

[$]Key Laboratory of Catalysis and Materials Science of the State Ethnic Affairs Commission and Ministry of Education, College of Chemistry and Material Science, South-Central University for Nationalities, Wuhan 430074, P. R. China

Supporting Information

ABSTRACT: Effects of chelating agents on the catalytic degradation of bisphenol A (BPA) was studied in the presence of $BiFeO_3$ nanoparticles as a heterogeneous catalyst and H_2O_2 as a green oxidant. The oxidizing ability of H_2O_2 in the presence of nano-$BiFeO_3$ alone was not so strong to degrade BPA at neutral pH values, due to the limited catalytic ability of nano-$BiFeO_3$. Once the surface of nano-$BiFeO_3$ was in situ modified by adding proper organic ligands, the BPA degradation was much accelerated in the pH range of 5−9. The enhancing effect of the ligand was observed to have an order of blank < tartaric acid < formic acid < glycine < nitrilotriacetic acid < ethylenediaminetetraacetic acid (EDTA). The addition of 0.25 mmol L^{-1} EDTA in the H_2O_2−$BiFeO_3$ system at pH 5.0 and 30 °C increased the BPA removal from 20.4% to 91.2% with reaction time of 120 min. The enhancing effect of the ligand was found to be indifferent of the possible dissolution of iron from nano-$BiFeO_3$, but correlated well with the accelerated •OH formation from the H_2O_2 decomposition at the $BiFeO_3$ surface, which was confirmed by ESR measurements and density functional theory studies. In general, more addition of EDTA, higher H_2O_2 concentrations, or higher temperatures were favorable to the BPA degradation. The effect of the EDTA addition on the kinetics of BPA degradation was also clarified.

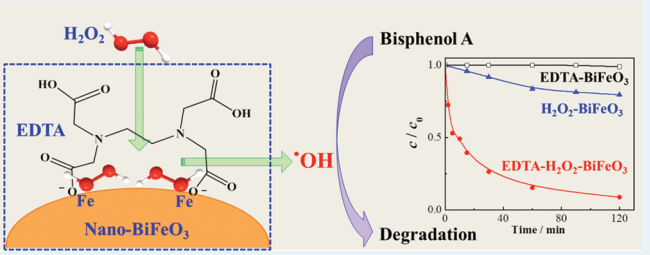

KEYWORDS: bisphenol A, $BiFeO_3$, ligand, catalytic degradation, surface modification

1. INTRODUCTION

Bisphenol A (2,2-bis(4-hydroxyphenyl) propane, abbreviated as BPA) is a xenobiotic that can be released into the environment from bottles, packaging, landfill leachates, paper, and plastics plants.[1] Because of its endocrine disrupting effect, BPA is acutely to aquatic organisms in the range of 1−10 mg L^{-1} for freshwater and marine species.[2] Thus, the development of methods to remove BPA is needed urgently. Biodegradation is an important step to detoxify BPA from the aquatic environment or aquatic organisms, but it requires a long time.[3] Also, it has been evidenced that BPA cannot be completely eliminated by the conventional treatment in drinking water supplies, and even it was reported that the treatment may produce byproduct with higher endocrine disrupting action.[4]

Advanced oxidation processes (AOPs), such as Fenton and Fenton-like processes, have been intensively investigated for the elimination of BPA. Torres et al. found that BPA (118 μmol L^{-1}) could be completely decomposed within 90 min in $FeSO_4$ solution (100 μmol L^{-1}) with continuous addition of H_2O_2 (119 μmol h^{-1}) at pH 3, but only 20% of total organic carbon (TOC) was eliminated even after 180 min.[5] Katsumata and co-workers observed that more than 90% of low level BPA (10 mg L^{-1}) was converted to CO_2 after 36 h in the UV−Fe^{2+} (0.4 mmol L^{-1})−H_2O_2 (4.0 mmol L^{-1}) at pH 4.0.[6] An integrated ultrasound−UV-Fe^{2+} (0.1 mmol L^{-1}) system was also developed to enhance the •OH generation, leading to BPA (118 μmol L^{-1}) could be completely mineralized to CO_2 at pH 3 after 3 h.[7] To overcome the demerit in the formation of a large amount of ferric hydroxide sludge in the homogeneous Fenton processes, iron oxides including hematite (α-Fe_2O_3),[8−10] maghemite (γ-Fe_2O_3),[9,10] lepidocrocite (γ-FeOOH),[11] and magnetite (Fe_3O_4)[8] were used instead of Fe^{2+}/Fe^{3+} ions as Fenton-like catalysts, but they often showed rather weak catalytic activity for the H_2O_2 activation. We found that the introduction of ultrasound irradiation into the H_2O_2−Fe_3O_4 system accelerated the degradation rate of Rhodamine B by 5.4 times at pH 5.0.[12] Several studies reported that the incorporation of V^{4+}, Co^{2+}, Mn^{2+},Ti^{4+}, Cr^{3+}, Si^{4+}, and Al^{3+} into the magnetite structure could increase the reactivity toward the H_2O_2 activation at dark.[13−17] To develop more efficient heterogeneous Fenton-like catalysts, we recently prepared $BiFeO_3$ nanoparticles and found that the nano-$BiFeO_3$ could efficiently catalyze the H_2O_2 decomposition to remove various organic pollutants including dyes and phenol.[18] However, it was observed

Received: May 31, 2011
Revised: July 25, 2011
Published: August 15, 2011

that $BiFeO_3$ nanoparticles were not valid for the BPA degradation in our preliminary experiments. It is necessary to increase further the catalytic ability of $BiFeO_3$ nanoparticles for the degradation of BPA in the presence of H_2O_2.

It is noticeable that the in situ addition of some chelating agents into the metal oxides dispersions can improve the photocatalytic behavior of the metal oxides. Rodríguez found that the addition of oxalic acid (0.2 mmol L^{-1}) to the UV−Fe_3O_4−H_2O_2 system increased the removal of BPA from 55.4% to 92.3% in 120 min.[8] Li et al. reported the beneficial effect of oxalate on the photodegradation of BPA over various iron oxides in the absence of H_2O_2, because both the dissolved and adsorbed Fe-oxalate complex exhibited strong ligand-to-metal charge transmitting (LMCT) bands in the near-UV and visible region, and could accelerate the formation of H_2O_2 and active radical species via a photo-Fenton like process.[9−11] We also found that such LMCT between colorless aromatic pollutants or hydroxycarboxylic acids to nano-TiO_2 could induce the photocatlaytic oxidation of organic substrates or reduction of the copresent Cr(VI) under the visible light illumination.[19,20] It was also reported that the ligand-enhanced oxidation rate of organic pollutants in the heterogeneous system of H_2O_2−Fe_3O_4 or O_2−zerovalent iron. This was explained by considering that the chelates could improve the dissolution of iron from the solid surface or limit iron precipitation, and then the propagation of homogeneous reaction by the dissolved iron-ligands accelerated the production of reactive oxidizing species.[21−23] Sun and Pignatello demonstrated that some organic compounds such as nitrilotriacetic acid (NTA), rhodizonic acid and gallic acid could produce soluble Fe^{3+}-complexes, which were capable of removing 2,4-dichlorophenoxyacetic acid in the presence of H_2O_2 at pH 6.[24] We also observed that the chelates such as oxalic acid, citric acid and ethylenediaminetetraacetic acid (EDTA) were capable of raising the reactivity of Fe^{2+} ions with O_2 to produce reactive oxygen species.[25] Since the catalytic ability of $BiFeO_3$ originate from the reaction of H_2O_2 with the surface iron elements,[18] it is anticipated that a suitable chelate may enhance the catalytic degradation of BPA over $BiFeO_3$ nanoparticles in the presence of H_2O_2. The goal of the present work is to study the effect of various organic ligands on the removal of BPA in the H_2O_2−$BiFeO_3$ system and clarify the kinetic pathway in BPA degradation in such a system.

2. EXPERIMENTAL SECTION

2.1. Chemical and Materials. $Fe(NO_3)_3 \cdot 9H_2O$, $Bi(NO_3)_3 \cdot 5H_2O$, and BPA were obtained from Tianjin Chemical (China). 2,2-Diphenyl-1-picryl-hydrazyl (DPPH) and 5,5-dimethyl-1-pyrroline-*N*-oxide (DMPO) were purchased from Aldrich. Other reagents were provided by Sinopharm Chemical Reagent Co., Ltd. (China). All chemicals were analytical grade reagents and were used as received without further purification. Milli-Q water was used in the experiments for the ion chromatography measurements, and double distilled water was used in all other test.

2.2. Catalytic Degradation of BPA. $BiFeO_3$ nanoparticles were prepared with a sol−gel method as described in our previous work.[18] The obtained $BiFeO_3$ nanoparticles had a highly crystalline and single-phase perovskite structure with grain sizes of 100−150 nm and BET specific surface area of 8.34 $m^2 g^{-1}$. In a typical catalytic experiment, $BiFeO_3$ nanoparticles (0.025 g) were dispersed into 50 mL of BPA aqueous solution (0.1 mmol L^{-1}) in the absence and presence of organic ligands (0.25 mmol L^{-1}) at pH 5.0 with sonication for 1 min. The tested chelates included formic acid, oxalic acid, tartaric acid, glycine, NTA and EDTA (cf. Supporting Information Table S1 for their structures). The mixture was magnetically stirred for 30 min to achieve the adsorption−desorption equilibrium of the concerned compounds on the catalyst. The degradation of BPA was initiated by rapid adding H_2O_2 to the above dispersions under magnetic stirring conditions. At given time intervals, aliquots (2 mL) of the reaction solution were sampled and filtered immediately through a 0.22 μm filter, and the concentrations of BPA and other concerned compounds in the filtrate were analyzed. The rapid filtering off the $BiFeO_3$ nanoparticles was very efficient for quenching the oxidation of BPA, and we found that the BPA concentration in the filtrate did not change after it was kept for 2 h at room temperature.

2.3. Analytical Methods. The concentration of BPA was determined with high performance liquid chromatography (HPLC) on a PU-2089 HPLC (JASCO, Japan), equipped with a Amethyst C18−P column (250 mm ×4.6 mm) and an UV detector (JASCO UV-2075). The mobile phase was a mixture of methanol and water (75/25, v/v) with a flow rate of 1.0 mL min^{-1}, and the UV detector was operated at 230 nm. The concentrations of EDTA and aliphatic acids were monitored on a Dionex ICS-1500 ion chromatography system equipped with the CD 25 conductivity detector, IonPac AS 23 (250 mm ×4 mm) analytical column, IonPac AG 23 (50 mm ×4 mm) guard column, and anion ASRS electrolytic suppressor (ASRS-ULTRA II, 4 mm, suppressor current of 70 mA). The mobile phase was 28 mmol L^{-1} KOH with a flow rate of 1.0 mL min^{-1}, and the injection volume was 20 μL.

The concentration of dissolved ferrous ion was measured with 1,10-phenantroline method by recording the absorbance at 510 nm. The sample (1.5 mL) was mixed with 0.3 mL water, 0.3 mL 1,10-phenanthroline (0.2%) and 0.4 mL sodium acetate (1.0 mol L^{-1}). Total dissolved iron was quantified after adding 0.3 mL hydroxylamine hydrochloride (10%) to 1.5 mL sample, and then mixed with 0.3 mL 1,10-phenanthroline (0.2%) and 0.4 mL sodium acetate (1.0 mol L^{-1}).

Active free radicals were identified with electron spin resonance (ESR) on a Bruker ESR 300E with a microwave bridge (receiver gain, 1×10^5; modulation amplitude, 2 G; microwave power, 10 mW; modulation frequency, 100 kHz). For the measurement, the samples (100 μL) were collected from the reaction solution after being reacted for 5 min, and immediately mixed with 20 μL DMPO (0.2 mol L^{-1}) to form DMPO-radicals adduct. Because of the instability in water solutions, the ESR signal of $O_2^{-\bullet}/HO_2\bullet$ was detected in dimethyl sulfoxide. The formation of •OH radicals was also evaluated by using coumarin as a fluorescence probe, which easily reacts with •OH to form highly fluorescent 7-hydroxycoumarin.[26] Instead of BPA, coumarin (1.0 mmol L^{-1}) was added into the systems of H_2O_2−$BiFeO_3$ or ligand−H_2O_2−$BiFeO_3$. The fluorescent intensity of generated 7-hydroxycoumarin was monitored at 456 nm with the excitation wavelength of 346 nm on a JASCO FP6200 spectrofluorometer.

ATR-FTIR analysis was carried out with a VERTEX 70 Micro Fourier Transform Infrared/Raman spectroscope equipped with a high sensitivity DLATGS detector and a horizontal ATR-FTIR attachment (Bruker, Germany). Density Functional Theory (DFT) method was employed to investigate the adsorption process of H_2O_2 on the surface of bared and ligand-adsorbed

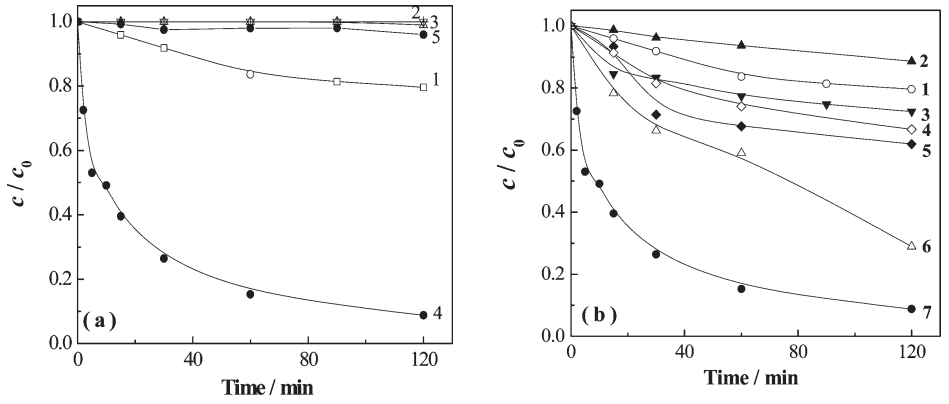

Figure 1. (a) Degradation of BPA in the systems of (1) H_2O_2−$BiFeO_3$, (2) H_2O_2−EDTA, (3) EDTA−$BiFeO_3$, (4) EDTA−H_2O_2−$BiFeO_3$, and (5) DPPH−EDTA−H_2O_2−$BiFeO_3$. (b) Degradation of BPA in the H_2O_2−$BiFeO_3$ systems without (1) and with the addition of ligands of (2) oxalic acid, (3) tartaric acid, (4) formic acid, (5) glycine, (6) NTA, and (7) EDTA. Unless otherwise stated, the basic reaction conditions were as follows: [$BiFeO_3$] = 0.5 g L^{-1}, $[BPA]_0$ = 0.1 mmol L^{-1}, $[H_2O_2]_0$ = 10 mmol L^{-1}, $[ligand]_0$ = 0.25 mmol L^{-1}, $[DPPH]_0$ = 5.0 μmol L^{-1} temperature 30 °C, pH 5.0.

$BiFeO_3$ in the Material Studio 4.4 software package. The configuration optimization was implemented by Vosko-Wilk-Nusair (VWN) functional of local density approximation (LDA) method with double numerical basis sets plus polarization function (DNP).[27] The core of Fe and Bi atoms were treated with effective core potentials (ECP), and the other atoms (containing O, H, C and N) were treated with all electron sets. To achieve the structure optimization, the convergence criteria of the SCF tolerance, the energy tolerance, the displacement tolerance and the maximum force tolerance were set to 2.0×10^{-6} eV/atom, 2×10^{-5} a.u., 5×10^{-4} nm, and 4×10^{-3} Ry/a.u., respectively. The remaining parameters were the default values.

3. RESULTS AND DISCUSSION

3.1. Enhanced Degradation of BPA by Ligands. Figure 1 illustrates the catalytic degradation of BPA (0.1 mmol L^{-1}) in the H_2O_2−$BiFeO_3$ system at pH 5.0 and 30 °C. It is easily seen that BPA can be slowly degraded over $BiFeO_3$ in the presence of H_2O_2, leading to a BPA removal of 20.4% within 120 min (curve 1 in Figure 1a). In contrast, no marked removing of BPA was observed in the systems of H_2O_2−EDTA and EDTA−$BiFeO_3$ (curves 2 and 3 in Figure 1a). When EDTA (0.25 mmol L^{-1}) was introduced into the H_2O_2−$BiFeO_3$ system, the degradation of BPA was significantly promoted (curve 4 in Figure 1a), resulting in a BPA removal of 91.2% within 120 min. Such enhancing effect was also observed when other organic ligands were added instead of EDTA. Except oxalic acid (OA), the addition of tartaric acid (TA), formic acid (FA), and glycine (Gly) and NTA all increased the degradation of BPA with the order of OA < blank < TA < FA < Gly < NTA < EDTA (Figure 1b). This suggests that the addition of favorable ligands indeed enhanced the catalytic ability of H_2O_2−$BiFeO_3$ system for the degradation of BPA.

However, the observed order of the enhancing effect of the chelating agents is quite different from that reported for heterogeneous Fenton or photo-Fenton systems. Li et al. found that the UV photocatalytic degradation of BPA in the iron oxide-carboxylic acids systems followed the order of blank < malic acid < malonic acid < TA ≪ citric acid ≪ OA, and concluded that the bicarboxylic acid with a shorter carbon chain in the presence of iron oxides might easily form a more stable Fe^{3+}-carboxylate complex with a higher photochemical activity than that with a longer carbon chain.[11] Xue et al. reported that the degradation of pentachlorophenol in the presence of microsized Fe_3O_4 and H_2O_2 by adding ligands had the sequence: OA > EDTA > citrate > tartrate > blank.[21] Keenan and Sedlak found NTA exhibited a better effect in improving the oxidant yield in the zerovalent iron/O_2 system than EDTA did.[23] To clarify the reasons for the observed enhancing order in the present work, it is necessary to reveal the fate of various ligands on the catalytic degradation of BPA in the system of H_2O_2−$BiFeO_3$.

3.2. Ligand-Induced Iron Dissolution Has No Effect on the BPA Degradation. In the previous reports,[21−23] the beneficial effect of ligands on the catalytic ability of iron-bearing powders was ascribed to that the chelating agents could increase the dissolution of iron by forming soluble iron complexes, thus the generated homogeneous Fenton reaction increase the production of reactive oxygen radicals. In order to confirm the contribution of homogeneous Fenton reaction, the amount of dissolved iron was measured during the catalytic degradation of BPA in the H_2O_2−$BiFeO_3$ system without and with the addition of ligands. Except for the addition of NTA, no Fe^{2+} ions were detected in the reaction media, because the dissolved Fe^{2+} was easily oxidized to Fe^{3+} in an oxidizing atmosphere containing abundant H_2O_2.[21] It was found that the iron leaching from $BiFeO_3$ nanoparticles was below the detection limit (i.e., 0.05 mg L^{-1}) in the absence of ligands, and the addition of the ligands generally increased the total dissolved iron in the solution (Supporting Information Figure S1), mainly because the iron-ligand complexing could strong accelerate the release and/or the reductive dissolution of iron oxide.[28] The amount of iron leaching had the order of blank, formic acid, glycine (less than 0.05 mg L^{-1}) < tartaric acid (0.41 mg L^{-1}), oxalic acid (0.43 mg L^{-1}) < EDTA (0.98 mg L^{-1}) < NTA (1.50 mg L^{-1}). This order of the Fe dissolution increasing is much different from that of the BPA degradation promotion arising from the addition of ligands, suggesting that the enhancing effect of ligands is not due to their promoting the dissolution of iron species from $BiFeO_3$ nanoparticles. Moreover, iron leaching solutions were prepared by incubating the catalyst (0.5 g L^{-1}) in 0.25 mmol L^{-1} of EDTA at pH 5.0 for 2 h and then removing the $BiFeO_3$ nanoparticles with a 0.22 μm filter. No BPA degradation was observed within 2 h after 0.1 mmol L^{-1} BPA and 10 mmol L^{-1} H_2O_2 were added into the leaching solution. These observations imply that the effect of chelating agents on the BPA degradation in H_2O_2−$BiFeO_3$ system cannot be attributed to the dissolved iron, but mainly to the heterogeneous

dx.doi.org/10.1021/cs2002862 |ACS Catal. 2011, 1, 1193–1202

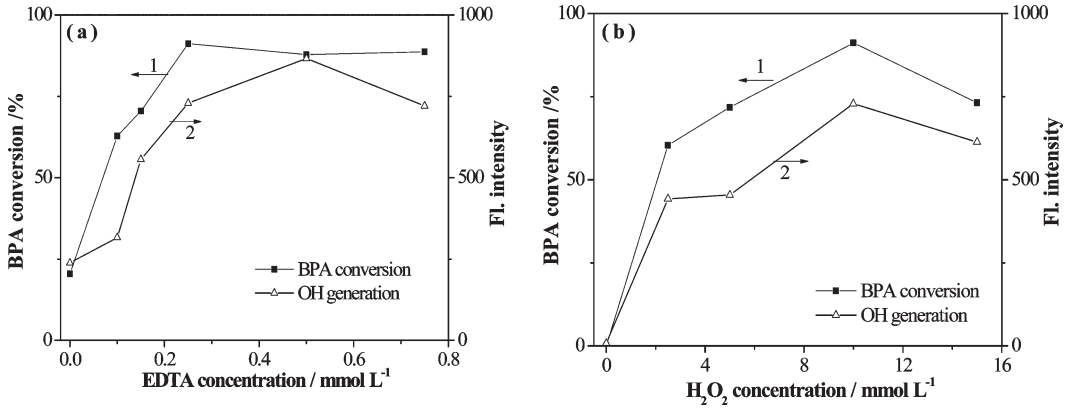

Figure 2. Effects of (a) EDTA concentration and (b) H_2O_2 concentration on (1) the BPA conversion within 120 min and (2) the fluorescent intensity of the solution with the addition of coumarin in the EDTA−H_2O_2−$BiFeO_3$ system within 30 min of reaction. The H_2O_2 concentration in (a) was 10.0 mmol L^{-1} and the EDTA concentration in (b) was 0.25 mmol L^{-1}.

Fenton reaction over the $BiFeO_3$ surface in situ modified with ligands, being different from that in the microsized Fe_3O_4−H_2O_2 system as reported by Xue el al.[21]

3.3. Effects of Reaction Conditions on BPA Degradation. The catalytic degradation of BPA in the ligand−H_2O_2−$BiFeO_3$ system was also influenced by reaction conditions, such as H_2O_2 concentration, ligand concentration, solution pH, and reaction temperature. Since EDTA is the most efficient chelating agent for the BPA removal among the tested ligand, further experiments were performed by using EDTA as the chelate. Because the BPA degradation in the H_2O_2−$BiFeO_3$ systems with and without the addition of EDTA did not follow a simple zero or first-order reaction process, the removal of BPA at a given reaction time was used to rationally evaluate the catalytic activity of as-prepared and surface-modified $BiFeO_3$ catalysts.

Figure 2a illustrates the effect of EDTA concentration on the BPA degradation in the EDTA−H_2O_2−$BiFeO_3$ system. As the initial concentration of EDTA was increased from 0 to 0.7 mmol L^{-1}, the BPA removal within 120 min was significantly increased from 20.4% in the absence of EDTA to 91.2% with adding 0.25 mmol L^{-1} of EDTA, and then approached an almost constant when the EDTA concentration was beyond 0.25 mmol L^{-1}. This is attributed to the double functions of EDTA. First, EDTA favors the H_2O_2 adsorption on the $BiFeO_3$ surface and the generation of •OH radicals being the main reactive oxidizing species (see section 3.5 for more discussions), promoting the BPA degradation. Second, EDTA as an organic compound reacts competitively with •OH radicals,[21,23,24] consuming •OH species available for the BPA degradation. To evidence this assumption, the •OH formation was quantitatively assessed by adding the fluorescent probe coumarin instead of BPA into the H_2O_2−$BiFeO_3$ system, where coumarin was oxidized by the •OH radicals to a strong fluorescent 7-hydroxycoumarin. As increasing reaction time, the fluorescence intensity reached a roughly constant value at ∼30 min (Figure 5c), thus, the fluorescence intensity at 30 min was used to evaluate the relative amount of •OH radicals. It was clearly showed that the amount of generated •OH radicals was increased by adding more EDTA, but an excessive EDTA inhibited the •OH formation in the H_2O_2−$BiFeO_3$ system (curve 2 in Figure 2a). Thus, 0.25 mmol L^{-1} is the optimal initial EDTA concentration for improving the catalytic degradation of BPA in the EDTA−H_2O_2−$BiFeO_3$ system.

At a given initial amount of EDTA (0.25 mmol L^{-1}), the BPA conversions with respect to different initial H_2O_2 concentration were shown in Figure 2b. If no initial H_2O_2 was present, BPA was hardly degraded in the EDTA-$BiFeO_3$ system, indicating that EDTA alone is not capable of promoting $BiFeO_3$ to produce enough amounts of reactive radical species. When the initial concentration of H_2O_2 was increased from 0 to 10.0 mmol L^{-1}, the BPA removal was increased from 0 to 91.2% (curve 1 in Figure 2b). However, an over high concentration of H_2O_2 was detrimental for the BPA degradation, because H_2O_2 also reacts with •OH without producing other oxidants. This can be further supported by the fact that the amount of generated •OH was significantly increased with the increase of H_2O_2 concentration in the range of 0−10 mmol L^{-1}, but then reduced when the H_2O_2 concentration was higher than 10.0 mmol L^{-1} (curve 2 in Figure 2b).

Figure 3a represented the effect of reaction temperature on the BPA degradation, which demonstrated that increasing temperature was favorable to enhancing the BPA degradation. For example, as the temperature was increased from 20 to 60 °C, the BPA removal within 30 min was increased from 5.4% to 23.0%, and 25.6% to 97.8% in the absence and presence of EDTA, respectively. At any tested temperature, the catalytic degradation of BPA in the presence of EDTA was much faster than that in the absence of EDTA, and the beneficial role of EDTA on the BPA removal became more effective at higher temperatures.

Solution pH is another important factor influencing the catalytic ability of $BiFeO_3$. In the H_2O_2−$BiFeO_3$ system, the BPA removal within 2 h was significantly decreased from 87.0% to 17.2% with increasing of pH from 3 to 9 (curve 1 in Figure 3b), being in good agreement with the pH dependence of RhB degradation in the H_2O_2−$BiFeO_3$ system.[18] In contrast, the addition of EDTA into the above system changed the trend for the pH effect on the BPA degradation. The BPA conversion within 120 min in the EDTA−H_2O_2−$BiFeO_3$ system first increased from 20.4% at pH 3 to 91.2% at pH 5 and then kept roughly a constant value. In fact, the removal of BPA (∼87.1 ± 2.9%) was almost insensitive to the solution pH in the range from pH 4 to 9 (curve 2 in Figure 3b). It was not that, although the presence of EDTA greatly increased the BPA removal at pH in the range from pH 4 to 9, the BPA removal at pH 3.0 with the addition of EDTA was much less than that without the addition of EDTA. Because the solution acidity at pH 3 is favorable to the dissolution of iron species from $BiFeO_3$ nanoparticles, the

dx.doi.org/10.1021/cs2002862 |ACS Catal. 2011, 1, 1193–1202

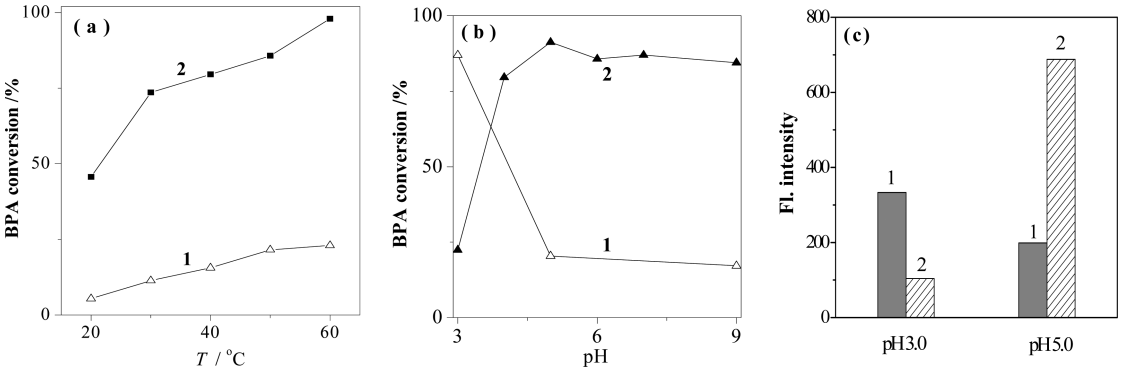

Figure 3. (a) Effect of temperature on BPA removal (within 30 min) in the systems of (1) H_2O_2−$BiFeO_3$ and (2) EDTA−H_2O_2−$BiFeO_3$ at pH 5.0. (b) Effect of pH on BPA conversion (within 120 min) in the (1) H_2O_2−$BiFeO_3$ and (2) EDTA−H_2O_2−$BiFeO_3$ systems at 30 °C. (c) Fluorescent intensity of the solution within 30 min of reaction after the addition of coumarin in the systems of (1) H_2O_2−$BiFeO_3$ and (2) EDTA−H_2O_2−$BiFeO_3$.

mentioned difference strongly demonstrates again that the enhancing effect of EDTA on the degradation of BPA is not related to the possible ligand-induced iron dissolution. In comparison with the case without EDTA, the lower BPA removal with the addition of EDTA at pH 3 is well correlated with the considerable depression of the generation of •OH with the addition of EDTA at pH 3.0, which was evidenced by the fact that the fluorescence intensity of 7-hydroxycoumarin was decreased from 333.1 in the coumarin−H_2O_2−$BiFeO_3$ system to 103.9 in the coumarin−EDTA−H_2O_2−$BiFeO_3$ system (Figure 3c).

3.4. New Type of Kinetics of BPA Degradation in the Presence of EDTA. It is known that a heterogeneous Fenton reaction is a pseudo-first-order reaction with respect to the concentration of BPA by assuming that the instantaneous concentration of oxidizing species is constant.[9−11] However, the BPA degradation in the H_2O_2−$BiFeO_3$ system, especially with the addition of EDTA, showed a very complex behavior: the BPA concentration was first decreased rapidly and then followed by a much slower degradation process. This led to that the BPA decay could be fitted by neither the zero-, first-, nor second-order kinetics. We conducted the degradation of BPA with the addition of EDTA at different concentrations (Supporting Information Figure S2). Intriguingly, it could be well curve-fitted to a triple exponential expression as given below (eq 1, $R^2 \geq 0.97$),

$$\frac{c_t}{c_0} = \sum_{i=1}^{n} a_i e^{-k_i t} \ (i = 1, 2, 3) \qquad (1)$$

where c_t and c_0 is the BPA concentration (mmol L^{-1}) at reaction time (min) of t and 0, respectively; a_i and k_i (i = 1, 2, and 3) represent the fraction coefficient and apparent rate constant (min^{-1}) of BPA degradation for the ith type of degradation, respectively. This suggests the overall degradation of BPA in the EDTA−H_2O_2−$BiFeO_3$ system is the combination of the three distinct pseudo-first-order catalytic processes with different degradation rates occurred simultaneously. We assumed that the three distinct catalytic processes correspond to that occurred at EDTA-adsorbed sites, freely active sites, and deactivated sites. Here, the so-called freely active sites mean the ones for the degradation of BPA on the surface of $BiFeO_3$ nanoparticles in the absence of EDTA, where the deactivated sites was the ones where the BPA degradation was hindered due to the competitively degradation or the blocking effect of generated intermediates.[29] According to the assumption of three parallel degradation processes, we have $a_1 + a_2 + a_3 = 1$. On the basis of the observed enhancing effect of EDTA, we know that the degradation of BPA at the EDTA-adsorbed sites (i = 1) is much faster than that occurs at the other two types of reaction sites. Because of the deleterious effect of the intermediate products, the BPA degradation at deactivated sites (i = 3) is much slower than that at the so-called free active sites (i = 2).

Table 1. Kinetic Parameters in eq 1 for the BPA Degradation over $BiFeO_3$ (0.5 g L^{-1}) in the Presence of 10.0 mmol L^{-1} H_2O_2 with Various Additions of EDTA at pH 5 and 30 °C

$c_{0,EDTA}$ (mmol L^{-1})	k_1 (min^{-1})	a_1	k_2 (min^{-1})	a_2	k_3 (min^{-1})	a_3	R^2
0	0	0	0.016	0.25	$<10^{-4}$	0.75	0.97
0.10	0.33	0.34	0.028	0.29	$<10^{-4}$	0.37	0.98
0.15	0.40	0.41	0.033	0.24	$<10^{-4}$	0.34	0.98
0.25	0.44	0.44	0.034	0.45	$<10^{-4}$	0.12	0.99
0.50	0.82	0.56	0.025	0.34	$<10^{-4}$	0.10	0.99
0.75	0.28	0.64	0.010	0.38	0	0	0.98

The obtained kinetic parameters in eq 1 are listed in Table 1. No matter with the addition of EDTA or not, the data fitting obtained that $k_3 < 10^{-4}$ min^{-1} in all the conditions, which demonstrates that the BPA degradation at the third type of sites is indeed very slow, being generally negligible in comparison with that at other two types of reaction sites. In the absence of EDTA, there are no EDTA-adsorbed sites on the surface of $BiFeO_3$ nanoparticles, and it is unnecessary to consider the first type of BPA degradation process, that is, $a_1 = 0$ and $k_1 = 0$ for the zero addition of EDTA. Under this condition, the apparent rate constant k_2 and its fraction a_2 was fitted to be 0.016 min^{-1} and 0.25, respectively. Similarly, the values of k_3 and a_3 were evaluated as $k_3 < 10^{-4}$ min^{-1} and $a_3 = 0.75$. This illustrates that in the case of no EDTA addition, the generated intermediates greatly hinders the degradation of the remained BPA. In fact, 75% of the added BPA was still present in the H_2O_2−$BiFeO_3$ system even after a reaction of 300 min. Moreover, we also carried the degradation reaction for 120 min and then redegraded the residual BPA by adding fresh $BiFeO_3$ (0.5 g L^{-1}) and a certain amount of H_2O_2 into the resultant intermediates-containing solution after the used $BiFeO_3$ nanoparticles were separated off by vacuum filtration with a 0.22 μm filter. It was observed that the further degradation of BPA was negligible in the recovered

dx.doi.org/10.1021/cs2002862 |ACS Catal. 2011, 1, 1193–1202

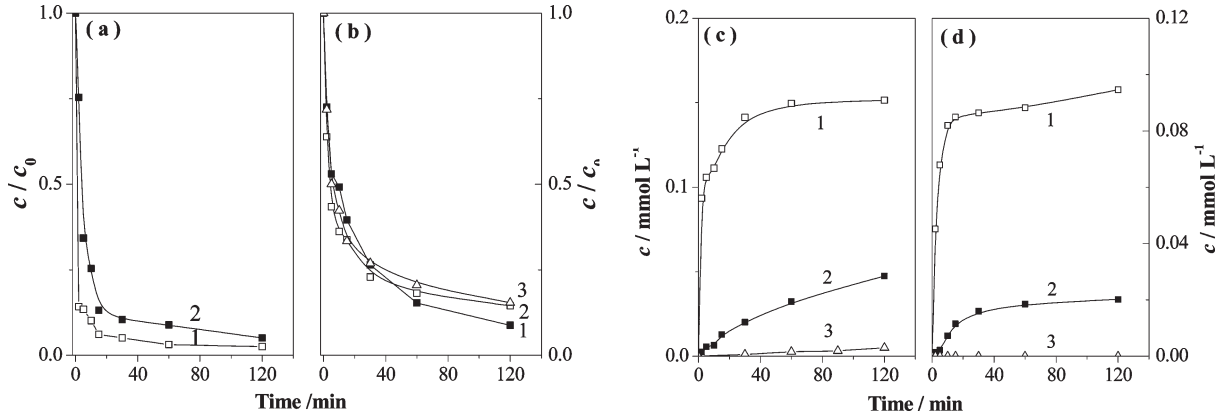

Figure 4. (a) EDTA degradation in systems of (1) H_2O_2−$BiFeO_3$ and (2) BPA−H_2O_2−$BiFeO_3$. (b) BPA degradation in the EDTA−H_2O_2−$BiFeO_3$ system without (1) and with addition of (2) 0.05 mmol L^{-1} formic acid and (3) 0.02 mmol L^{-1} IMDA. (c, d) Generation of (c) formic acid and (d) IMDA in systems of (1) EDTA−H_2O_2−$BiFeO_3$, (2) BPA−EDTA−H_2O_2−$BiFeO_3$, and (3) BPA−H_2O_2−$BiFeO_3$.

solution with the newly addition of fresh $BiFeO_3$ and H_2O_2. When the used $BiFeO_3$ (0.5 g L^{-1}) was reused as the catalyst for the degradation of fresh BPA (0.1 mmol L^{-1}) in the presence of 10 mmol L^{-1} of fresh H_2O_2, the BPA removal was as low as 17% within 120 min (Supporting Information Figure S3). These further confirmed that the generated intermediates are very harmful to the catalytic degradation of BPA in the H_2O_2−$BiFeO_3$ system.

When EDTA was added, the adsorption of EDTA on the surface of $BiFeO_3$ nanoparticles significantly enhanced the generation of •OH radicals, thus, a much larger value of k_1 was observed in the degradation process. With increasing the EDTA addition, the BPA degradation at the EDTA-adsorbed sites on the surface of $BiFeO_3$ nanoparticles generally became more and more important. For example, by increasing the addition of EDTA from 0.10 to 0.25 and 0.50 mmol L^{-1}, the apparent rate constant k_1 was increased from 0.33 to 0.44 and then 0.82 min^{-1}, and the a_1 value representing the contribution of the BPA degradation over the EDTA-adsorbed sites of $BiFeO_3$ was roughly enlarged from 34% to 44%, and then 56%. Relative to the significantly increasing in k_1 values, the absolute change in k_2 values were negligible in the presence of EDTA relative to that in the absence of EDTA (Table 1, Supporting Information Figure S2b). It was noted that the increased addition of EDTA resulted in significantly decreasing of the a_3 value, suggesting the deactivation of $BiFeO_3$ for the BPA degradation was depressed in the presence of EDTA.

To better understand the three distinct kinetic processes, the degradation of EDTA as a side reaction was also investigated. As shown in Figure 4a, accompanying the BPA removal, EDTA itself was rapidly degraded in the H_2O_2−$BiFeO_3$ system containing both EDTA and BPA, but being somewhat slower than that in the system of H_2O_2−$BiFeO_3$ alone. This indicates that there is a competition between BPA and EDTA for consuming the oxidizing species. Moreover, several aliphatic acids were formed during the simultaneous degradation of BPA and EDTA in the H_2O_2−$BiFeO_3$ system, and the main intermediates were proved to be formic acid and iminodiacetic acid (IMDA) (Supporting Information Figure S4) with an accumulated amount of 0.05 mmol L^{-1} and 0.02 mmol L^{-1} within 120 min, respectively (curves 2 in Figures 3c and 3d). If EDTA was absent in the H_2O_2−$BiFeO_3$ system, only 0.005 mmol L^{-1} of formic acid was detected during the BPA degradation (curves 3 in Figure 4c and 4d). In contrast, much more formic acid and IMDA were detected in the EDTA-H_2O_2−$BiFeO_3$ system without BPA (curves 1 in Figure 4c and 4d), suggesting that formic acid and IMDA mainly originated from the oxidation of EDTA. Similar intermediates were observed in the EDTA oxidation by the TiO_2 photocatalytic system or zerovalent iron/air system.[30,31] However, when either 0.05 mmol L^{-1} formic acid or 0.02 mmol L^{-1} IMDA was added into the BPA−EDTA−H_2O_2−$BiFeO_3$ system, the removal of BPA was slightly decreased by 5% (curves 2 and 3 in Figure 4b). Thus, the small values of k_3 should not be attributed to the accumulation of unfavorable intermediates from the codegradation of EDTA. In other word, the EDTA-adsorbed and bared sites on the $BiFeO_3$ surface are mainly responsible for the faster and slower degradation processes of BPA, respectively, while the very slow degradation of BPA at the third type of sites was still attributed to the harmful effect of the intermediates from the BPA degradation itself.

3.5. Ligand-Enhanced •OH Formation. The above results showed that the addition of favorable ligands greatly enhanced heterogeneous catalytic degradation of BPA in the H_2O_2−$BiFeO_3$ system. Since the possible ligand-induced iron dissolution has no effect on the BPA removal, the modified surface of $BiFeO_3$ by the ligand was studied with the ATR-FTIR technology. We recorded the FTIR spectra of $BiFeO_3$ powders before and after the immersion treatment in ligand solutions for 2 h, and found that both EDTA and oxalic acid could be adsorbed on the $BiFeO_3$ surface, as signified by the main spectral bands of carboxyl group at 1611 and 1393 cm^{-1} for EDTA, and at 1630 and 1316 cm^{-1} for oxalic acid (Supporting Information Figure S5). Moreover, the asymmetric vibration of carboxyl group ($\nu_{as(COO-)}$) in the spectra of ligand-adsorbed $BiFeO_3$ was shifted to higher wavenumbers by ~7−8 cm^{-1} in comparison with that of pure EDTA and oxalic acid, indicating the formation of a direct bonding between O atom of the carboxyl group of ligand and the Fe atom on the $BiFeO_3$ surface, which will shorten the C═O bond and increase $\nu_{as(COO-)}$.[32] Such interaction between the chelating agent and $BiFeO_3$ would change the chemical environment of the iron elements and/or adsorbed H_2O_2 on the $BiFeO_3$ surface, and consequently affect the H_2O_2 decomposition and the formation of the reactive oxygen radicals, which was further evidenced with ESR measurements by the addition of the spin trapping agent DMPO.

As shown in Figure 5a and 5b, the 4-fold characteristic peak with an intensity ratio of 1:2:2:1 is attained to DMPO−•OH adduct, whereas the sextet characteristic peak is attributed to

dx.doi.org/10.1021/cs2002862 |ACS Catal. 2011, 1, 1193–1202

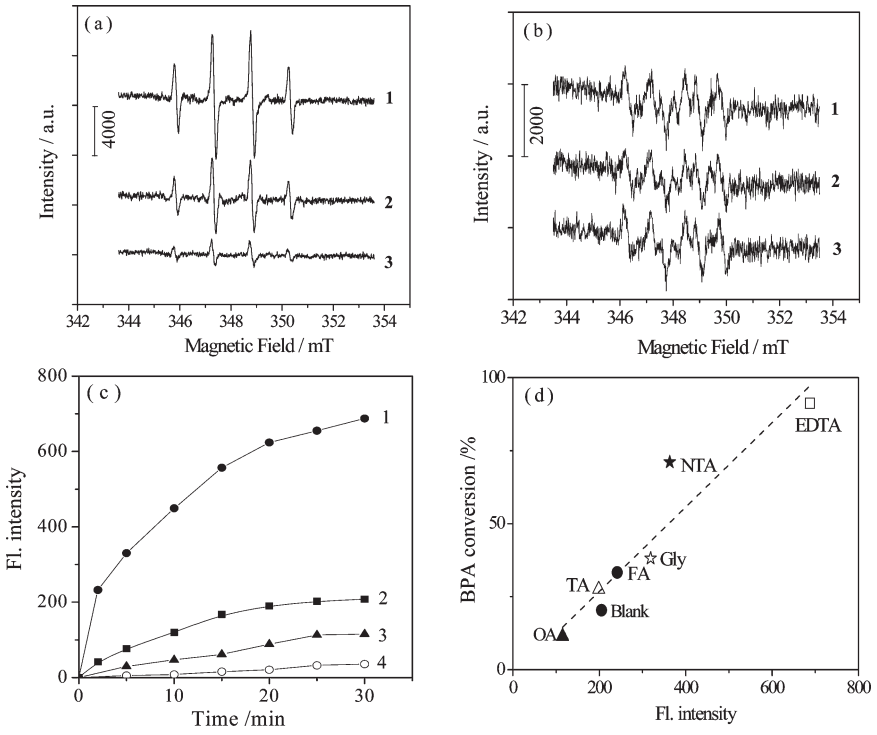

Figure 5. DMPO spin-trapping ESR spectra of (a) •OH radicals and (b) $O_2^{-\bullet}/HO_2\bullet$ in systems of (1) EDTA−H_2O_2−$BiFeO_3$, (2) H_2O_2−$BiFeO_3$, and (3) OA−H_2O_2−$BiFeO_3$. (c) Effect of reaction time on the fluorescent intensity of the coumarin solution in systems of (1) EDTA−H_2O_2−$BiFeO_3$, (2) H_2O_2−$BiFeO_3$, (3) OA−H_2O_2−$BiFeO_3$, and (4) DPPH−EDTA−H_2O_2−$BiFeO_3$. (d) The relationship between the BPA conversion within 120 min and the fluorescent intensity of the coumarin solution within 30 min in the H_2O_2−$BiFeO_3$ systems with and without the addition of ligands.

DMPO−$O_2^{-\bullet}/HO_2\bullet$ adduct. In our previous work, we observed that •OH radicals were the main reactive species for the RhB degradation by using $BiFeO_3$ nanoparticles and H_2O_2.[18] By comparing the ESR spectra in Figure 5a and 5b, it was found that $BiFeO_3$ could catalyze the H_2O_2 decomposition to produce a great amount of •OH radicals but not $O_2^{-\bullet}/HO_2\bullet$ species. The peak intensity of DMPO−•OH in the tested systems were ranked as OA−H_2O_2−$BiFeO_3$ < H_2O_2−$BiFeO_3$ < EDTA−H_2O_2−$BiFeO_3$, suggesting that the •OH formation was greatly enhanced by the addition of EDTA, but significantly depressed by adding oxalic acid. In contrast, the addition of chelates had a negligible effect on the formation of $O_2^{-\bullet}/HO_2\bullet$ radicals.

A coumarin fluorescent probe was used to quantitatively assess the •OH formation from H_2O_2 catalyzed by $BiFeO_3$ nanoparticles in the presence of various ligands. When coumarin instead of BPA was added into the H_2O_2−$BiFeO_3$ system, the oxidation of coumarin by •OH radicals produced fluorescent 7-hydroxycoumarin, leading to increasing of the fluorescence intensity with increasing reaction time until reaching a maximum at ca. 30 min (Figure 5c). Compared with the coumarin−H_2O_2−$BiFeO_3$ system, the presence of EDTA significantly accelerate the formation of 7-hydroxycoumarin, whereas the addition of oxalate had an obvious depression effect, being agreement well with the ESR results. At a given reaction time of 30 min, the fluorescence intensity in the tested systems was increased with the order of oxalic acid < blank, tartaric acid < formic acid < glycine < NTA < EDTA, being roughly consistent with the order of BPA conversion (Figure 5d). To verify the contribution of •OH radicals, a small amount of DPPH (5.0 μmol L^{-1}) as an •OH radicals scavenger was introduced into the coumarin−EDTA−H_2O_2−$BiFeO_3$ system, the generation of 7-hydroxycoumarin was almost completely inhibited (curve 4 in Figure 5c). If 5.0 μmol L^{-1} of DPPH (being 5% of BPA addition) was added into the system of BPA−EDTA−H_2O_2−$BiFeO_3$, a depressing effect of DPPH on the BPA degradation was also significant (curve 5 in Figure 1a). These phenomena indicates that •OH radicals are the dominant oxidizing species for the degradation of BPA in the H_2O_2−$BiFeO_3$ system, and the effect of the ligands on the BPA degradation are well correlated with their effect on the generation of •OH radicals. Moreover, the above suggestion was further supported by the similar trends in the BPA conversion and •OH formation with respect to different concentrations of either EDTA or H_2O_2 as shown in Figure 2.

To gain further insights into the effect of the ligands on the H_2O_2 decomposition and •OH formation, density functional theory (DFT) calculations were conducted to obtain the adsorption model of H_2O_2 and the interaction between ligands and $BiFeO_3$. Herein, EDTA and oxalate were selected as the typical chelates, because the former is the most efficient accelerating agent, while the latter is an inhibitor. The DFT analysis shows that H_2O_2 prefers to adsorb at the hollow site of $BiFeO_3$ facets which constitute of four Fe atoms (Figure 6a), and the interaction between O atom of H_2O_2 and Fe atoms would stretch the O−O bond of H_2O_2,[18] being favorable to the generation of •OH radicals as demonstrated by the ESR results and the fluorescence probing techniques. If EDTA or oxalic acid is present, then EDTA or oxalic acid is adsorbed on the $BiFeO_3$ surface through one of carboxyl groups (Figure 6b and 6c). Because of the larger spatial structure, the adsorbed EDTA has the ability to form a cave with a volume of 94.1 $Å^3$ on the surface $BiFeO_3$, while the molecular volume of H_2O_2 is ~30.0 $Å^3$, implying that two H_2O_2 molecules can be included to the $BiFeO_3$ surface by one EDTA

dx.doi.org/10.1021/cs2002862 |ACS Catal. 2011, 1, 1193–1202

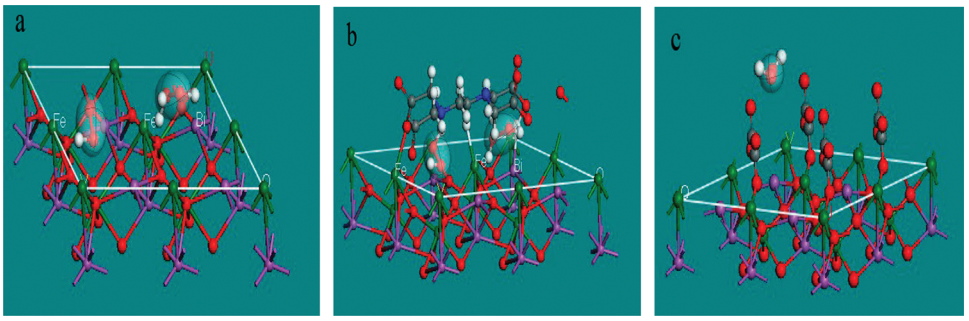

Figure 6. Images of H_2O_2 adsorption configuration on the surface of (a) bared, (b) EDTA−adsorbed and (c) OA−adsorbed $BiFeO_3$ nanoparticles. The white, red, green, purple, and blue spheres stand for H, O, Fe, Bi, and N atoms, respectively.

molecule (Figure 6b). It can be conceivable that the local concentration of H_2O_2 in the cave is higher compared to that on the bared $BiFeO_3$ surface, increasing their encounter frequency in the confined volume.[33] Besides, the physical properties of H_2O_2 are likely to differ in the confined volume, and the hydrogen bonding between the H atom of H_2O_2 and the N atom or carboxyl group of EDTA would further lower the electron density of O−O bond of H_2O_2, being favorable to the breakage of H_2O_2 to produce •OH. In contrast, the adsorbed oxalic acid on the $BiFeO_3$ surface failed to form the larger cave, and then reduce the surface Fe sites available for the interactions with H_2O_2, leading to an inactivation of $BiFeO_3$ surface (Figure 6c). Indeed, if 0.1 mmol L^{-1} of oxalic acid was added into the BPA−EDTA−H_2O_2−$BiFeO_3$ system, the BPA removal during 60 min was decreased from 84.8% to 57.2%, further supporting that the strong adsorption of oxalic acid decrease the affinity of $BiFeO_3$ for H_2O_2 molecule even in the coexistence of EDTA, and then greatly inhibited the H_2O_2 decomposition to produce •OH for attacking BPA.

3.6. Mechanism for the Enhanced BPA Degradation by Ligand Addition. Based on the above discussions, the catalytic degradation of BPA over $BiFeO_3$ in the presence of H_2O_2 with and without the chelating agent was illustrated in the following eqs 2−12, where the values in the parentheses of eqs 2,[34] 3,[34] 5a,[21] 5b,[35] 9,[36] and 10[36] are the second order rate constants. (For eq 4, see ref 35.)

$$\equiv Fe^{3+} + (H_2O_2)s \rightarrow \equiv Fe^{2+} + {\bullet}HO_2 + H^+ (0.003 M^{-1} s^{-1}) \quad (2)$$

$$\equiv Fe^{2+} + (H_2O_2)_s \rightarrow \equiv Fe^{3+} + {\bullet}OH + OH^- \ (40 - 80 M^{-1} s^{-1}) \quad (3)$$

$${\bullet}HO_2 \rightleftarrows O_2^{-\bullet} + H^+ \ (pK_a = 4.8) \quad (4)$$

$$\equiv Fe^{3+} + O_2^{-\bullet} \rightarrow \equiv Fe^{2+} + O_2 \ (1.4 \times 10^5 \ M^{-1} s^{-1} \ for Fe^{3+}) \quad (5a)$$

$$\equiv Fe^{3+} + {\bullet}HO_2 \rightarrow \equiv Fe^{2+} + O_2 + H^+ \ (3.5 \times 10^5 M^{-1} s^{-1} \ for Fe^{3+}) \quad (5b)$$

$$\equiv Fe^{3+}{-}L + (H_2O_2)_s \rightarrow \equiv Fe^{2+}{-}L + {\bullet}HO_2 + H^+ \ (L = ligand) \quad (6)$$

$$\equiv Fe^{2+}{-}L + (H_2O_2)_s \rightarrow \equiv Fe^{3+}{-}L + {\bullet}OH + OH^- \quad (7)$$

$$\equiv Fe^{3+}{-}L + O_2^{-\bullet} \rightarrow \equiv Fe^{2+}{-}L + O_2 \quad (8)$$

$$Fe^{3+}{-}EDTA + O_2^{-\bullet} \rightarrow \equiv Fe^{2+}{-}EDTA + O_2 \ (2.0 \times 10^6 \ M^{-1} s^{-1}) \quad (9)$$

$$Fe^{2+}{-}EDTA + H_2O_2 \rightarrow \equiv Fe^{3+}{-}EDTA + {\bullet}OH + OH^- \ (2.0 \times 10^4 \ M^{-1} s^{-1}) \quad (10)$$

$$BPA + {\bullet}OH \rightarrow \ldots \rightarrow CO_2 + H_2O \quad (11)$$

$$L + {\bullet}OH \rightarrow \ldots \rightarrow CO_2 + H_2O \quad (12)$$

As proposed in our previous report,[18] the catalytic decomposition of H_2O_2 by $BiFeO_3$ may involve the initial adsorption of H_2O_2 on the surface bound Fe^{3+} (namely, $\equiv Fe^{3+}$), followed by the production to $\equiv Fe^{2+}$ and $O_2^{-\bullet}/HO_2{\bullet}$ radicals. The generated $\equiv Fe^{2+}$ can react with adsorbed H_2O_2 to generate •OH radicals, whereas the $\bullet HO_2$ radicals may further reduce $\equiv Fe^{3+}$ to $\equiv Fe^{2+}$. Relative to the slow reaction of $\equiv Fe^{3+}$ with H_2O_2 (eq 2), the generated $\bullet HO_2$ radicals might be mainly consumed in the effective reduction of $\equiv Fe^{3+}$ so that few $O_2^{-\bullet}/HO_2{\bullet}$ radicals were detected in the ESR measurements (eqs 5a and 5b); however, this process will consume the added H_2O_2. In the presence of ligands, the strong complexing ability makes the chelating agents to easily adsorb on the surface $\equiv Fe^{3+}$ sites, which may affect the catalytic activity of $BiFeO_3$ in the following possible three ways: (1) by its competition with target pollutants for consuming the oxidizing species; (2) by changing the affinity of iron for the H_2O_2 adsorption; and (3) by ligand field effects on the redox properties of the iron.[24] The first factor is supported by the effects of ligand concentration on the degradation rate of BPA and the formation rate of •OH radicals (Figure 2a). Also, the co-oxidation of ligand resulted in that the three distinct catalytic processes with different degradation rates occurred in the overall degradation of BPA as discussed in section 3.4. Second, although it is generally accepted that the presence of ligand might reduce the surface sites available for the H_2O_2 adsorption,[21] the DFT analysis suggested some chelating agents like EDTA could form a larger cave at the $BiFeO_3$ surface than the molecular volume of H_2O_2, and then enhance the local concentration of H_2O_2 in the confined cave. Moreover, it has reported the complex of Fe^{3+}/Fe^{2+} with ligand decreased the Fe^{3+}/Fe^{2+} redox potential (e.g., from 0.77 to 0.356, 0.256, and 0.209 V (vs NHE) for NTA, OA, and EDTA, respectively[37]), enhancing the thermodynamic

dx.doi.org/10.1021/cs2002862 |ACS Catal. 2011, 1, 1193–1202

driving force for the Fenton reaction. In addition, the reduction rate constant of Fe^{3+} with $O_2^{-\bullet}/HO_2\bullet$ is influenced by adding ligand, for example, it is significantly increased from 1.4(or 3.5) $\times 10^5$ M^{-1} s^{-1} in the absence of EDTA to 2×10^6 M^{-1} s^{-1} in the presence of EDTA (eqs 5a, 5b, and 9), and thus it is expected to improve the overall reaction rate. Because the effect of ligand was an integrated contribution from the above three factors and there is a lack of thermodynamic and structural data on the complexes, it is difficult to clearly reveal the fate of various ligands on the H_2O_2 decomposition and the •OH formation. However, the overall effect of the chelating agents whether it is to improve the BPA degradation or not is dependent on the net amount of generated •OH radicals as shown in Figure 5. The addition of suitable ligands such as glycine, NTA and EDTA can significantly the •OH generation and the BPA degradation, whereas the addition of oxalic acid greatly suppress the •OH formation, and then inhibited the BPA degradation. Moreover, the beneficial effect of ligands was affected by the initial concentration of ligands, solution pH, and reaction temperature.

4. CONCLUSIONS

The $BiFeO_3$ nanoparticles possess a fairly weak catalytic ability for the oxidation of refractory organic pollutants, leading to a removal of 20.4% of BPA (0.1 mmol L^{-1}) within 2 h in the presence of 0.5 g L^{-1} of $BiFeO_3$ and 10.0 mmol L^{-1} of H_2O_2 at pH 5 and 30 °C. To enhance the catalytic ability of $BiFeO_3$, in situ surface modification by ligands was developed in the present work. The BPA removal was found to be accelerated by adding chelates such as tartaric acid, formic acid, glycine, NTA and EDTA in a wide pH range from 4 to 9. Among the tested ligand, EDTA is the most efficient chelating agent, and the addition of 0.25 mmol L^{-1} EDTA led to a BPA removal of 91.2% under the same reaction conditions. The BPA degradation was dependent on the amount of added EDTA, the initial concentration of H_2O_2, solution pH, and reaction temperature. Moreover, the addition of EDTA strongly influenced the kinetic behavior of BPA degradation, originating from the three distinct reaction sites on the $BiFeO_3$ surface, that is, EDTA-adsorbed sites, bared $BiFeO_3$ sites, and intermediate-blocked sites. On the basis of the iron leaching, ESR, and density functional theory studies, the beneficial effect of ligand on the BPA degradation was confirmed to be governed by its reactivity for enhancing the •OH formation but irrelevant to the amount of iron dissolution.

■ ASSOCIATED CONTENT

Supporting Information. Figures depicting the iron leaching in the systems, catalytic degradations of BPA, effect of initial concentration of EDTA, degradation kinetics, ion chromatograms, and ATR-FTIR spectra. These materials are available free of charge via the Internet at http://pubs.acs.org.

■ AUTHOR INFORMATION

Corresponding Author

*Tel.: +86 27 87543432; fax: +86 27 87543632; E-mail: lhzhu63@yahoo.com.cn (L.Z.); hqtang62@yahoo.com.cn (H.T.).

■ ACKNOWLEDGMENT

Financial support by the National Science Foundation of China (grants Nos. 21077037 and 20877031) is gratefully acknowledged.

■ REFERENCES

(1) Staples, C. A.; Dom, P. B.; Klecka, G. M.; O'Block, S. T.; Harris, L. R. *Chemosphere* **1998**, *36*, 2149–2173.
(2) Kang, J.-H.; Kondo, F.; Katayama., Y. *Toxicology* **2006**, *226*, 79–89.
(3) Kang, J.-H.; Katayama, Y.; Kondo, F. *Toxicology* **2006**, *217*, 81–90.
(4) Hu, J.-Y.; Aizawa, T.; Ookubo, S. *Environ. Sci. Technol.* **2002**, *36*, 1980–1987.
(5) Torres, R. A.; Abdelmalek, F.; Combet, E.; Pétrier, C.; Pulgarin, C. *J. Hazard. Mater.* **2007**, *146*, 546–551.
(6) Katsumata, H.; Kawabe, S.; Kaneco, S.; Suzuki, T.; Ohta, K. *J. Photochem. Photobiol. A: Chem.* **2004**, *162*, 297–305.
(7) Torres, R. A.; Pétrier, C.; Combet, E.; Moulet, F.; Pulgarin, C. *Environ. Sci. Technol.* **2007**, *41*, 297–302.
(8) Rodríguez, E.; Fernández, G.; Ledesma, B.; Álvarez, P.; Beltrán, F. J. *Appl. Catal. B: Environ.* **2009**, *92*, 240–249.
(9) Li, F. B.; Li, X. Z.; Li, X. M.; Liu, T. X.; Dong, J. *J. Colloid Interface Sci.* **2007**, *311*, 481–490.
(10) Li, F. B.; Li, X. Z.; Liu, C. S.; Li, X. M.; Liu, T. X. *Ind. Eng. Chem. Res.* **2007**, *46*, 781–787.
(11) Li, F. B.; Chen, J.; Liu, C. S.; Dong, J. J.; Liu, T. X. *Biol. Fertil. Soils* **2006**, *42*, 409–417.
(12) Wang, N.; Zhu, L. H.; Wang, M. Q.; Wang, D. L.; Tang, H. Q. *Ultrason. Sonochem.* **2010**, *17*, 78–83.
(13) Deng, J. H.; Jiang, J. Y.; Zhang, Y. Y.; Lin, X. P.; Du, C. M.; Xiong, Y. *Appl. Catal. B: Environ.* **2008**, *84*, 468–473.
(14) Costa, R. C. C.; Lelis, M. F. F.; Oliveira, L. C. A.; Fabris, J. D.; Ardisson, J. D.; Rios, R. R. V. A.; Silva, C. N.; Lago, R. M. *J. Hazard. Mater.* **2006**, *B129*, 171–178.
(15) Chen, D.; Liang, X. L.; Qin, Z. H.; Fan, M. D.; Zhu, J. X.; Yuan, P. *Appl. Catal. B: Environ.* **2009**, *89*, 527–535.
(16) Magalhães, F.; Pereira, M. C.; Botrel, S. E. C.; Fabris, J. D.; Macedo, W. A.; Mendonc, R.; Lago, R. M.; Oliveira, L. C. A. *Appl. Catal. A: Gen.* **2007**, *332*, 115–123.
(17) Pham, A. L. T.; Lee, C.; Doyle, F. M.; Sedlak, D. L. *Environ. Sci. Technol.* **2009**, *43*, 8930–8935.
(18) Luo, W.; Zhu, L. H.; Wang, N.; Tang, H. Q.; Cao, M. J.; She, Y. B. *Environ. Sci. Technol.* **2010**, *44*, 1786–1791.
(19) Wang, N.; Zhu, L. H.; Deng, K. J.; She, Y. B.; Yu, Y. M.; Tang, H. Q. *Appl. Catal. B: Environ.* **2010**, *95*, 400–407.
(20) Wang, N.; Zhu, L. H.; Huang, Y. P.; She, Y. B.; Yu, Y. M.; Tang, H. Q. *J. Catal.* **2009**, *266*, 199–206.
(21) Xue, X.; Hannaa, K.; Despasa, C.; Wu, F.; Deng, N. *J. Mol. Catal. A: Chem.* **2009**, *311*, 29–35.
(22) Sanchez, I. S.; F.; Font, J.; Fortuny, A.; Fabregat, A.; Bengoa, C. *Chemosphere* **2007**, 338–344.
(23) Keenan, C. R.; Sedlak, D. L. *Environ. Sci. Technol.* **2008**, *42*, 6936–6941.
(24) Sun, Y. F.; Pignatello, J. J. *J. Agric. Food Chem.* **1992**, *40*, 322–327.
(25) Luo, W.; Abbas, M. E.; Zhu, L. H.; Zhou, W. Y.; Li, K. J.; Tang, H. Q.; Liu, S. S.; Li, W. Y. *Anal. Chim. Acta* **2009**, *640*, 63–67.
(26) Guan, H. M.; Zhu, L. H.; Zhou, H. H.; Tang, H. Q. *Anal. Chim. Acta* **2008**, *608*, 73–78.
(27) Vosko, S. H.; Wilk, L.; Nusair, M. *Can. J. Phys.* **1980**, *58*, 1200–1211.
(28) Blesa, M. A.; Borghi, E. B.; Maroto, A. J. G.; Regazzoni, A. E. *J. Colloid Interface Sci.* **1984**, *98*, 295–305.
(29) Fuente, L.; de la; Acosta, T.; Babay, P.; Curutchet, G.; Candal, R.; Litter, M. I. *Ind. Eng. Chem. Res.* **2010**, *49*, 6909–6915.
(30) Babay, P. A.; Emilio, C. A.; Ferreyra, R. E.; Gautier, E. A.; Getter, R. T.; Litter, M. I. *Water Sci. Technol.* **2001**, *44*, 179–185.

(31) Zhou, T.; Lim, T.-T.; Lu, X. H.; Li, Y. Z.; Wong, F.-S. *Sep. Purif. Technol.* **2009**, *68*, 367–374.
(32) Guan, X.-H.; Chen, G.-H.; Shang, C. *J. Environ. Sci.* **2007**, *19*, 438–443.
(33) Du, Y. K.; Rabani, J. *J. Phys. Chem. B* **2006**, *110*, 6123–6128.
(34) Mazille, F.; Schoettl, T.; Pulgarin, C. *Appl. Catal. B: Environ* **2009**, *89*, 635–644.
(35) Lin, S.-S.; Gurol, M. D. *Environ. Sci. Technol.* **1998**, *32*, 1417–1423.
(36) Kwon, B. G.; Kim, E. J.; Lee, J. H. *Chemosphere* **2009**, *74*, 1335–1339.
(37) Strathmann, T. J.; Stone, A. T. *Environ. Sci. Technol.* **2002**, *36*, 5172–5183.